JMEPEG (2012) 21:382–387
DOI: 10.1007/s11665-011-9934-z

1059-9495/$19.00

Effect of Martensite Morphology on Tensile Deformation of Dual-Phase Steel

E. Ahmad, T. Manzoor, M.M.A. Ziai, and N. Hussain

(Submitted September 17, 2010; in revised form March 15, 2011)

Three morphologies of martensite in dual-phase microstructure of 0.2% C steel were obtained by different heat treatment cycles. These morphologies consisting of grain boundary growth, scattered laths, and bulk form of martensite have their distinct patterns of distribution in the matrix (ferrite). In tensile testing martensite particles with these distributions behaved differently. A reasonable work hardening was gained initially during plastic deformation of the specimens. The control on ductility was found to depend on the alignment of martensite particles along the tensile axes. The increased surface area contact of martensite particles with ferrite, in grain boundary growth and scattered lath morphologies, facilitated stress transfer from ductile to hard phase. The ductility in the later part of deformation was dependent on the density of microvoids in the necked region. The microvoids are formed mostly by de-cohesion of martensite particles at the interface. The fracture of martensite particles is less prominent in the process of microvoid formation which predicts high strength of martensite.

Keywords dual-phase steel, heat treatment, microstructure, tensile properties

1. Introduction

Dual-phase steels (DPSs) are important member of high strength low alloy (HSLA) class of materials due to their good combinations of strength and ductility (Ref 1-4). The enhancements in formability with these strength and ductility combinations make DPS as strong candidates for structural applications. The increased strength to weight ratio of DPS provides an additional advantage in automobile industry as compared to conventional steel. This enhances the fuel economy and making DPS as useful candidate for automobile applications. The microstructures of DPS consist of a soft ductile ferrite matrix and 20-30% volume fraction of hard phase (martensite).

For the attainment of desired mechanical properties with DPS microstructure, a balance in volume fraction of martensite, its morphology and process of hot working in the intercritical region are the important parameters to be considered. A reasonable enhancement in tensile properties was obtained by employing thermomechanical processing with the development of substructure in ferrite and fiber morphology of martensite in the microstructure (Ref 5-7). This improvement in tensile properties was due to well alignment of martensite fibers with tensile axes to receive stresses from soft ferrite matrix.

The morphologies of martensite particles in ferrite matrix can also be changed by heat treatment cycles. Different combinations of strengths and ductilities were obtained with these morphologies in dual-phase microstructures (Ref 8, 9). In tensile testing low carbon martensite particles are plastically deformed before fracture and play a vital role in controlling the ductility of DPS (Ref 5, 8). In the present work, the straining behaviors were observed with different morphologies of high carbon martensite. With the intention to get better combinations of strengths and ductilities, these morphologies in dual-phase microstructure were employed to examine the tensile deformation behavior. In dual-phase steels ductilities during tensile deformations are controlled by the formations of microvoids. These microvoids are formed by de-cohesion at the ferrite-martensite interface and by fracture of martensite particles (Ref 7, 9, 10). The phenomenon of microvoid formation was examined in context with deformation in the necked region and its effect on control of ductility.

E. Ahmad, T. Manzoor, M.M.A. Ziai, and **N. Hussain**, Materials Division, PINSTECH, P. O. Nilore, Islamabad, Pakistan. Contact e-mail: dr.eahmad@yahoo.com.

2. Experimental Procedure

The chemical composition of A516 steel used is shown in Table 1. The material was provided in the form of hot rolled 12-mm thick slabs. The metallographic examination in as-received conditions revealed banded ferrite and pearlite microstructure, shown in Fig. 1. These rolling bands of prior deformation were removed by annealing at 1150 °C for 3 h followed by furnace cooling.

In order to establish the intercritical annealing temperature (ICAT) region of the steel, about 5-mm thick specimens were sliced from the slab and intercritically annealed at different temperatures ranging from 730 to 830 °C and quenched in iced brine solution. On the basis of these initial findings, a temperature of 750 °C, with the intentions of about 50% of austenite, was selected for further intercritical heat treatments. Three heat treatment cycles were followed to obtain different morphologies of martensite in the dual-phase microstructures. The schedules of these heat treatment cycles are schematically

Table 1 Chemical composition (wt.%) of as-received material

C	Mn	Si	S	P	Fe
0.20	0.90	0.22	0.04	0.035	Bal.

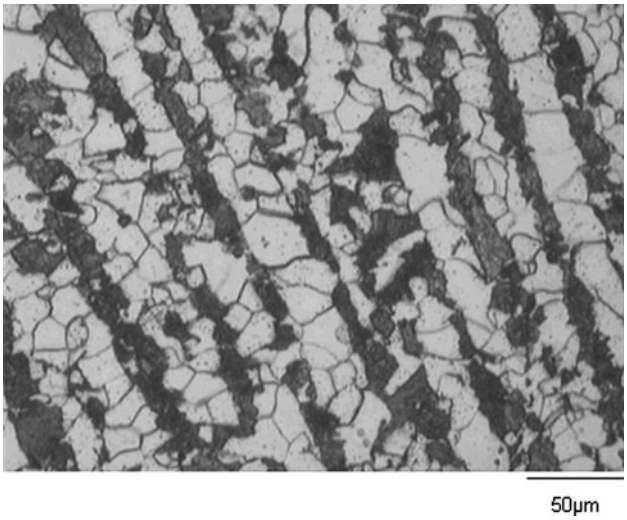

Fig. 1 Ferrite-pearlite microstructure of as-received steel

presented in Fig. 2. After homogenization at 1100 °C, the specimens were air cooled (AC), fast cooled (FC) by water quenching, and step cooled (SC) to intercritical temperature. The specimens were intercritically annealed at 750 °C and quenched in water with the intension to transform 50% of austenite to martensite.

Round tensile specimens were machined from the heat-treated slabs. The tensile testing was conducted on Instron testing machine model 4204 at room temperature with a cross-head speed of 2 mm/min.

All the specimens were etched in 2% nital solution for optical examination of microstructure and for microvoids observation on scanning electron microscope (SEM). Point counting technique was employed for quantitative phase measurements of ferrite and martensite.

3. Results and Discussion

3.1 Volume Fraction of Martensite with Intercritical Temperature Annealing

Figure 3 shows the changes in the volume fraction of martensite with increase in the intercritical temperatures. In the process of annealing all the specimens were quenched in the iced brine solution at approximately −5 °C with the intension to promote complete transformation of austenite to martensite. Similar trend of increase of volume fraction of austenite with intercritical temperatures were observed by other investigators (Ref 11-13). They have reported negligible amount of epitaxial growth of ferrite during quenching in iced brine solution. Therefore, it is assumed that volume fraction of martensite in Fig. 2 is near to the volume fraction of austenite, predicting the ICAT range of this steel. In the present investigation, 50% of

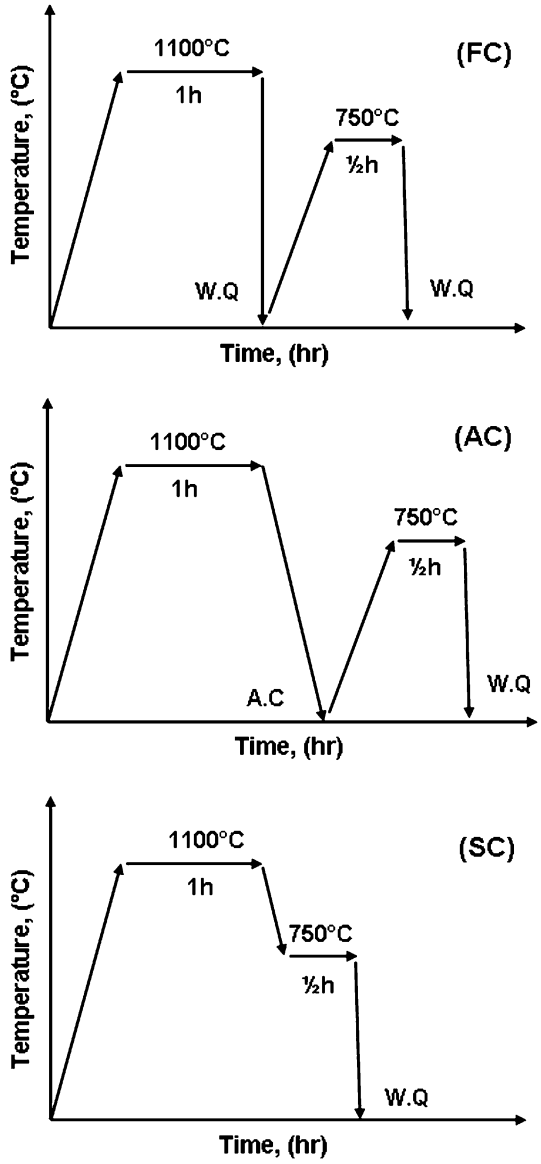

Fig. 2 Schedule of heat treatment cycles applied to obtain different morphologies of martensite in dual-phase microstructure

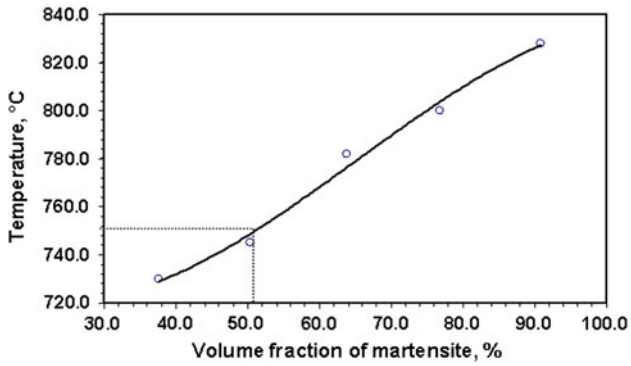

Fig. 3 Dependence of volume fraction of martensite on intercritical temperatures

martensite was obtained at ICAT of 750 °C which is lower than previous findings of Sarwar and Priestner (Ref 12) and Ahmad and Priestner (Ref 13). This reflects high hardenability of the

steel used in present investigation due to comparatively its higher carbon content.

3.2 Microstructural Development by Intercritical Annealing

Figure 4 shows three different morphologies of martensite obtained by heat treatment cycles of AC, FC, and SC. In AC cycle air cooling from austenite temperature, ferrite and pearlite microstructure was obtained at room temperature. Annealing at intercritical temperature of 750 °C would have promoted nucleation of austenite grains on the existing ferrite/carbide interface. Quenching in water resulted in connected network morphology of martensite in the ferrite matrix. For FC water quenching from austenite region resulted in fully martensite structure. Intercritical annealing with this starting microstructure, ferrite and austenite were grown by carbon diffusion to austenite. Quenching from the intercritical temperature resulted martensite grains with scattered lath morphology. In SC cycle of annealing, on slow cooling from austenite region ferrite grains were nucleated and grown from the austenite phase. Water quenching produced martensite with blocky-shaped morphology of particles embedded in soft ferrite grains. The grain coarsening of the ferrite and martensite in this part of heat treatment cycles may be due to slow cooling from austenite phase to intercritical region.

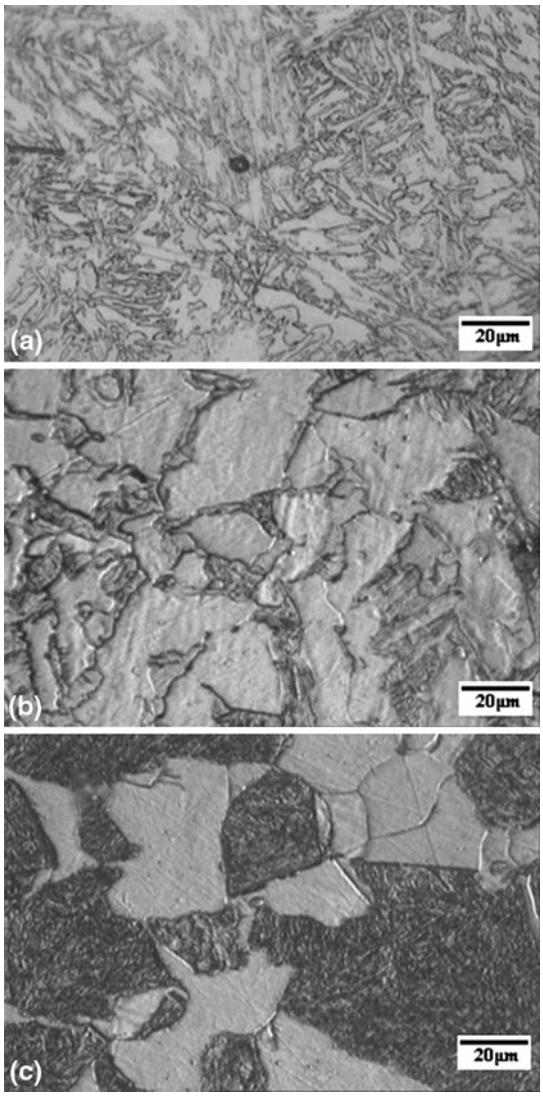

Fig. 4 Different morphologies of martensite in dual-phase microstructure, resulted by changing heat treatment cycles (a) FC, laths of martensite (b) AC, grain boundary growth (c) SC, bulk growth

The formations of austenite at temperatures between 740 and 900 °C were studied by Speich et al. (Ref 14) in a series of 1.5 wt.% Mn steels containing 0.06-0.20 wt.% C. With starting microstructure of ferrite and pearlite, they observed that the growth of austenite into ferrite, at low temperatures (750 °C), was controlled by manganese diffusion in ferrite, which is much easier along the grain boundaries. Therefore, preferential direction of austenite growth must be parallel to the grain boundaries. This model of formation of austenite can easily explain the distribution of martensite along the ferritic grain boundaries as described in AC cycle of heat treatment.

For connected network and blocky-shaped morphologies of martensite Sarwar et al. (Ref 9) adopted a series of intercritical heat treatment cycles. However, in the present AC and SC cycles, presented recently by Park et al. (Ref 8), these morphologies were obtained by uncomplicated ways of heat treatments. The hard laths of martensite evenly distributed in soft matrix of ferrite, as in FC, can behave like whiskers in a metal matrix composite.

3.3 Tensile Properties

The tensile data with three morphologies of martensite are presented in Table 2. The carbon contents of martensite were estimated from the approximate carbon content of ferrite (0.01%), the carbon content of steel (0.2%), and volume fraction of martensite. With a decrease in volume fraction of martensite its carbon contents are increased that may be resulted in probable enhancement in strength of this phase. The true stress-true strain curves, to the onset of necking with continuous deformation behavior of DPS are shown in Fig. 5. The continuous yielding phenomenon of DPSs is well explained with generation of dislocations during volume

Table 2 Tensile data with distinct morphologies of martensite in dual-phase steels

Specimen code	Martensite, %	Carbon content of martensite	Max. true stress, MPa	True uniform strain, %	Total elongation, %	UTS, MPa	Uniform elongation, %	0.2% Proof stress, MPa
FC	47	0.41	643	15	22	560	14	336
AC	46	0.42	686	17	27	585	16	394
SC	49	0.40	1065	8	9	980	9	595
0.09C steel (5)	42					779	9.0	
0.17C 50% rolled steel (6)	49					872	9.2	

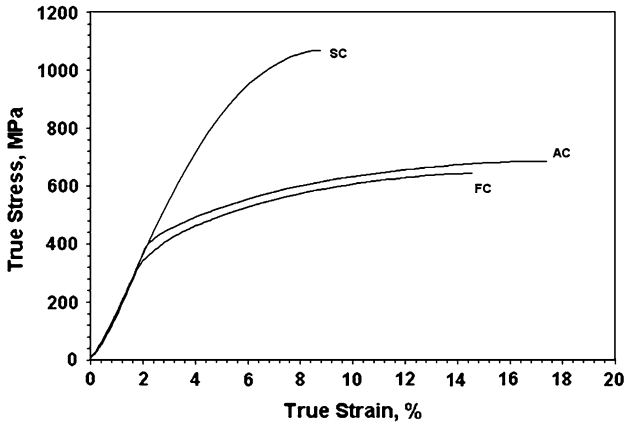

Fig. 5 True stress-true strain curves with three morphologies of martensite: FC, AC, and SC. The smooth yielding reflects a typical tensile deformation behavior of dual-phase steels

expansion associated with austenite to martensite transformation. This expansion linked with austenite to martensite transformation also develops stresses in ferrite (Ref 15, 16) adjacent to the martensite. In the presence of these stresses and abundant of unobstructed mobile dislocations, yielding phenomenon is smooth and starts at low stress levels (Ref 1). The interaction of these dislocations with each other and with fine dispersion of secondary phase results in high work hardening. However, the work hardening process of dual-phase steels is complex and it was previously defined in three stages of plastic deformation (Ref 17, 18).

(a) The first stage (0.1-0.5% strain) shows rapid work hardening, because of the elimination of residual stresses and rapid build up of back stress due to plastic incompatibility of two phases.
(b) In the second stage (0.5-4% strain), the work hardening rate of ferrite is reduced because the plastic flow of the ferrite is constrained by the hard, undeforming martensite particles. In actual practice DPSs show a remarkable decrease in work hardening rate, passing through this stage of plastic deformation. Therefore, plastic flow of ferrite would have not been retarded by martensite particles; rather stress transfer from ferrite to martensite helps the plastic flow of the ferrite.
(c) Finally, in the third stage (4-18% strain), dislocation cell structures are formed, and further deformation in the ferrite is governed by dynamic and cross-slip and by eventual yielding of the martensite phase.

In the present case true stress-true strain curves, Fig. 5 showed a delayed start of first stage of plastic deformations. Similarly, the work hardening in second stage is pursued by AC and FC with connected and dispersed morphologies of martensite, while SC remained in elastic stage of deformations containing blocky shape of martensite. In view of these deviations from previously defined stages of deformations following two factors appeared to be considered:

- Carbon content of steel and martensite. With high carbon content of martensite, ranging from 0.40 to 0.42% (Table 2), more stresses are introduced in the ferrite during phase transformation. The process of elimination of these stresses is completed with more plastic straining of ferrite. Previously, with low carbon content of steel (0.09 wt.%) these stages were followed during plastic deformation (Ref 7).
- The morphology of transformed martensite in the ferrite matrix plays a vital role in straining of ferrite (Ref 8). As martensite remains un-deformed in the initial stages of straining an equiaxed martensite would be less efficient than with elongated morphology in receiving stresses from ferrite. The fibrous morphology of martensite in ferrite matrix, developed by thermomechanical process of rolling, showed an enhancement in tensile properties (Ref 5, 11). This was reported as a result of an increase in surface area of two phases to ease the stress transfer from ductile ferrite to hard martensite particles.

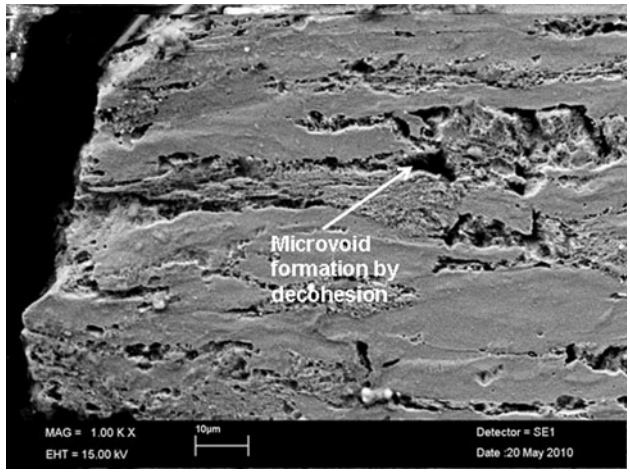

Fig. 6 Microvoid formation mainly by de-cohesion of martensite particle in FC. The rupture of martensite is less visible near fracture surface, predicting its high strength

In view of these observations, plastic straining in AC and FC started late but continued with sufficient work hardening. With bulk morphology of martensite, SC gained the same work hardening rate but straining of ferrite and also of martensite in later stages of deformation. Therefore, martensite particles in SC would have not been aligned near fracture to receive stresses from ferrite, resulted in minimum plastic deformation. The tensile data of previous studies with low carbon content of steel and martensite (Ref 5, 6) are also included in Table 2. In "not rolled" condition (Ref 5) the strength and ductility are less comparable than present findings of tensile properties. Thermomechanical process of 50% rolling reduction resulted in an increase in UTS owing to the development of substructure in the ferrite (Ref 6). However, an appreciable loss in ductility reflects that a hard ferrite with substructure development was not as efficient as in AC, FC, or SC for stress transfer to martensite during tensile deformation.

3.4 Tensile Fracture

Fractured tensile specimens of AC, FC, and SC were studied on SEM for evaluation of their fracture mechanism. Figures 6 to 8 show the microstructural examination in the necked region of three martensite morphologies. Microvoids were developed in this region, predominantly in AC & FC specimens, and their coalescence promoted the ultimate failure. In DPSs, microvoids

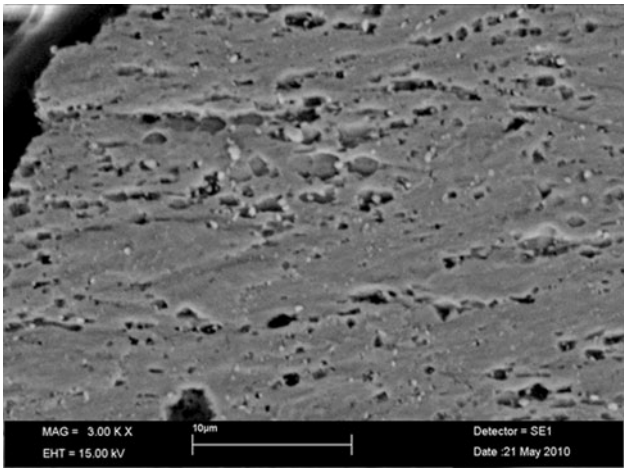

Fig. 7 Microvoid concentration in the necked region near fracture surface in AC. This predicts the localized nature of necking with ample plastic deformation

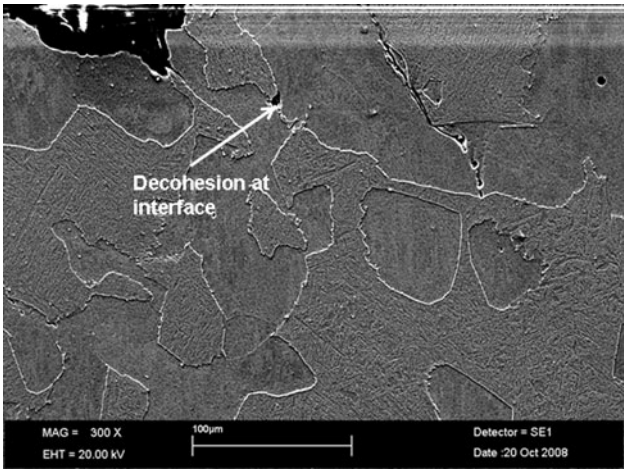

Fig. 8 Microvoid formation by de-cohesion at interface with minimum of martensite deformation in SC. The poor alignment of martensite particles along the tensile axes resulted in minimum gain of ductility near fracture

near the fracture surface are formed either by fracture of martensite particle or by de-cohesion at the ferrite-martensite interphase. Stenbruner et al. (Ref 19) observed that in dual-phase steels, with 0.08% C, microvoids are concentrated near the fracture in localized necking and a uniform distribution in defused necking. A high population of microvoids near fracture surface with stretched microstructure along the tensile axes shows a localized nature of necking in AC and FC. The stretched morphology of microstructure near the fracture is due to well alignment of martensite particles along the tensile force. The maximum ductility gained in this later part is by plastic deformation of ferrite and it is due to better stress transfer from ferrite to martensite (Ref 5, 7). The minimum of plastic deformation along with poor alignment of martensite particles to receive the stresses from ferrite is visible in SC (Fig. 8). De-cohesion at martensite-ferrite interface is dominant feature for microvoid formation predicting the brittle nature of martensite particles.

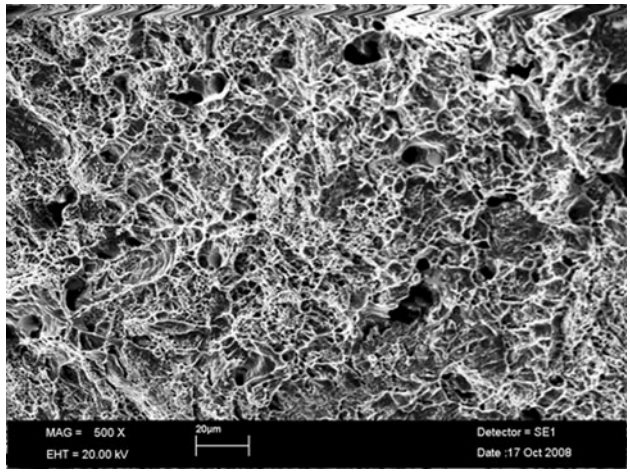

Fig. 9 Fracture surface with dimples, showing typical ductile nature of deformation in FC

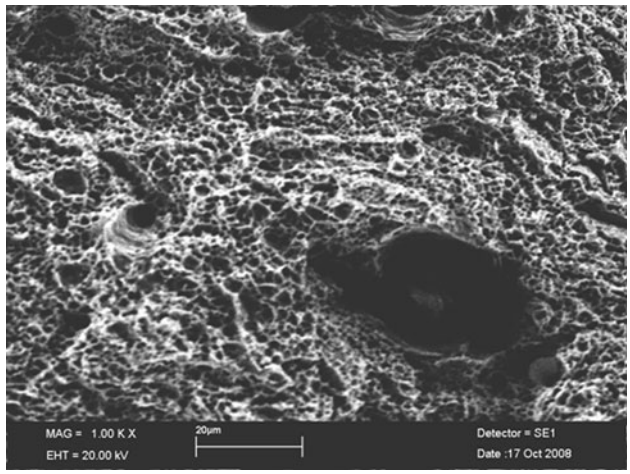

Fig. 10 Fracture surface with ductile dimples of AC. The high concentration of microvoids near fracture resulted in ductile nature of tensile fracture

Previously with different morphologies, martensite particles are plastically deformed in the later part of tensile testing (Ref 5, 8). This may be due to low carbon contents of steel and martensite because strength of martensite is largely dependent on its carbon content. Comparatively high carbon contents of steel and of martensite in SC, the plastic deformation near fracture advanced with minimum of plastic flow of martensite particles. The reduced plastic deformation of martensite resulted in less available area of contact of two phases for better stress transfer from ferrite to martensite.

The fracture surface of AC, FC, and SC specimens are shown in Figs. 9 to 11. Ductile dimples with minimum display of brittle failure through cleavage were observed in AC and FC. This reflects that stresses were fairly transferred from ferrite to martensite particles during plastic deformation and ferrite remained soft to promote ductile failure. On the other hand in SC, the process of work hardening would have developed dislocations and resulting stresses in the ferrite were accumulated till the fracture by the development of cleavage facets, Fig. 11. These cleavages facets clearly defined the brittle mode

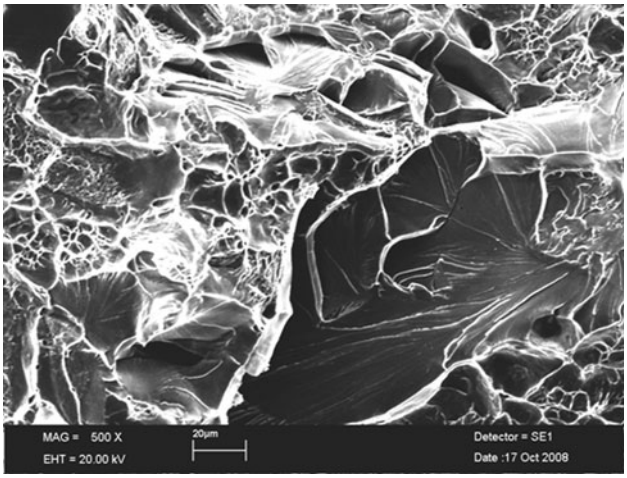

Fig. 11 Fracture surface showing predominantly with cleavage facets in SC. A minimum gain of ductility resulted in brittle nature of fraction

of fracture in SC. Previously, thermomechanical processing in intercritical region ferrite becomes considerably hard by substructure development, but it deformed with ductile dimples appearance on the fracture surface (Ref 5, 7, 11). The martensite with fibrous morphology was reported to be involved in receiving stresses from ferrite for deformation in ductile fashion. These observations clearly support the fact that in dual-phase steels near fracture morphologies of individual phases (ferrite + martensite) play an important role in defining the ultimate failure mode in tensile testing.

4. Conclusions

- Three distinct morphologies of martensite in the dual-phase microstructure were obtained by changing heat treatment cycles. These morphologies, defined as grain boundary connected, scattered laths and bulk form of martensite were explicit to the starting microstructure in the intercritical region. With the starting microstructures of ferrite plus pearlite and full martensite, grain boundary growth and laths morphologies were, respectively, acquired as a result of intercritical annealing. While the bulk morphology of martensite was attained by growth on the existing austenite grain boundaries.
- In tensile properties observations plastic straining started at different stress levels with sufficient work hardening rates. However, specimens with grain boundary growth and lath morphologies of martensite gained improved ductility than with bulk growth. Martensite particles alignment with tensile axes and also sufficient area exposure to the ferrite provided better stress transfer arrangements from ductile to hard phase.
- Microstructure observations near fracture clearly revealed that specimen with bulk morphology of high carbon martensite particles have minimum of plastic deformation. Very few microvoids were formed by de-cohesion at the interface resulting in brittle failure by cleavage facets appearance on the fracture surface. In grain boundary growth and scattered morphologies the martensite particles near fracture are better aligned for proper stress transfer from ferrite to martensite. Microvoids are concentrated in the necked regions and with their coalescence ductile dimples appeared on the fracture surfaces.

References

1. M.S. Rashid, Relationship Between Steel Microstructure and Formability, *Formable HSLA and Dual-Phase Steels*, A.T. Davenport, Ed., AIME, New York, 1977, p 1–24
2. G.R. Speich and R.L. Miller, Mechanical Properties of Ferrite-Martensite Steels, *Structure and Properties of Dual Phase Steels*, A.T. Davenport, Ed., TMS-AIME, New York (NY), 1979, p 145–182
3. S.S. Hansen and R.R. Pradhan, Structure/Property Relationship and Continuous Yielding Behavior in Dual-Phase Steels, *Proceedings Fundamentals of Dual-Phase Steels*, R.A. Kot and B.L. Bramfitt, Ed., AIME, New York, 1981, p 113–144
4. N.K. Balliger and T. Gladman, Work Hardening of Dual-Phase Steels, *Met. Sci.*, 1981, **15**(3), p 95–108
5. E. Ahmad, T. Mazoor, N. Hussain, and N.K. Qazi, Effect of Thermomechanical Processing on Hardenability and Tensile Fracture of Dual-Phase Steel, *Mater. Des.*, 2008, **29**, p 450–457
6. M. Sarwar and R. Priestner, Influence of Ferrite-Martensite Microstructural Morphology on Tensile Properties of Dual-Phase Steel, *J. Mater. Sci.*, 1996, **31**, p 2091–2095
7. E. Ahmad, T. Mazoor, and N. Hussain, Thermomechanical Processing in the Intercritical Region and Tensile Properties of Dual Phase-Steel, *Mater. Sci. Eng. A*, 2009, **508**, p 259–265
8. K.S. Park, K.T. Park, D.L. Lee, and C.S. Lee, Effect of Heat Treatment Path on the Cold Formability of Drawn Dual-Phase Steel, *Mater. Sci. Eng. A*, 2007, **449–451**, p 1135–1138
9. M. Sarwar, T. Manzoor, E. Ahmad, and N. Hussain, The Role of Connectivity of Martensite on Tensile Properties of a Low Alloy Steel, *Mater. Des.*, 2007, **28**, p 1928–1933
10. M. Erdogan and S. Tekeli, The Effect of Martensite Particle Size on Tensile Fracture of Surface Carburized AISI, 8620 Steel with Dual Phase Core Microstructure, *Mater. Des.*, 2002, **23**, p 597–604
11. S. Sun and M. Pugh, Properties of Thermomechanically Processed Dual-Phase Steels Containing Fibrous Martensite, *Mater. Sci. Eng.*, 2002, **335**(1–2), p 298–308
12. M. Sarwar and R. Priestner, Hardenability of Austenite in a Dual-Phase Steel, *J. Mater. Eng. Perform.*, 1999, **8**(3), p 380–384
13. E. Ahmad and R. Priestner, Effect of Rolling in the Intercritical Region on the Tensile Properties of Dual-Phase Steel, *J. Mater. Eng. Perform.*, 1998, **7**(6), p 772–776
14. G.R. Speich, V.A. Demarest, and R.L. Miller, Formation of Austenite During Intercritical Annealing of Dual-Phase Steels, *Metall. Trans. A*, 1981, **12**, p 1419–1428
15. C.L. Magee and R.G. Davies, On the Volume Expansion Accompanying the fcc and bcc Transformation in Ferrous Alloys, *Acta Metall.*, 1972, **20**, p 1031–1043
16. J.M. Moyer and G.S. Ansell, The Volume Expansion Accompanying the Martensite Transformation in Iron-Carbon Alloys, *Metall. Trans. A*, 1975, **6**, p 1785–1791
17. J. Gerbase, J.D. Embury, and R.M. Hobbs, The Mechanical Behavior of Some Dual Phase Steels with Emphasis on the Initial Work Hardening Rate, *Structures and Properties of Dual Phase Steels*, R.A. Kot and J.W. Morris, Ed., TMS-AIME, Warrendale, PA, 1979, p 118–143
18. J.M. Rigsbee and P.J. VaderArendm, Laboratory Studies of Microstructures and Structure-Property Relationships in "Dual Phase" HSLA Steels, *Formable HSLA and Dual-Phase Steels*, A.T. Davenport, Ed., AIME, New York, 1977, p 56–86
19. D.L. Steinbrunner, D.K. Matlock, and G. Krauss, Void Formation During Tensile Testing of Dual-Phase Steels, *Metall. Trans. A*, 1988, **19**, p 579–589